Articles

Influence of Bulky N-Substituents on the Formation of Lanthanide Triple Helical Complexes with a Ligand Derived from Bis(benzimidazole)pyridine: Structural and Thermodynamic Evidence

Gilles Muller,[†] Jean-Claude G. Bünzli,*[,†] Kurt J. Schenk,[‡] Claude Piguet,[§] and Gérard Hopfgartner[||]

The Institute of Inorganic and Analytical Chemistry, BCH, and the Institute of Crystallography, BSP, University of Lausanne, CH-1015-Lausanne, Switzerland, Department of Inorganic, Analytical and Applied Chemistry, Sciences II, University of Geneva, CH-1211 Geneva-4, Switzerland, and Pharma Division, Hoffmann-La Roche, CH-4070 Basle, Switzerland

Received November 14, 2000

The planar aromatic tridentate ligand 2,6-bis(1-*S*-neopentylbenzimidazol-2-yl)pyridine (L^{11}) reacts with Ln(III) (Ln = La−Lu) in acetonitrile to give the successive complexes $[Ln(L^{11})_n]^{3+}$ ($n = 1-3$). However, stability constants determined by spectrophotometry and NMR titrations show that formation of the tris complexes is not favored, log K_3 being around 1 for La(III) and Eu(III), while no such species could be evidenced for the smaller Lu(III) ion. The X-ray structures of L^{11} (monoclinic, $P2_1$, $a = 13.4850(12)$ Å, $b = 12.0243(11)$ Å, $c = 16.4239(14)$ Å, $\beta = 103.747(7)°$), $[La(ClO_4)_2(L^{11})_2]_3[La(ClO_4)_2(H_2O)(L^{11})_2](ClO_4)_4 \cdot 15MeCN$ (**1a**, monoclinic, $P2_1$, $a = 21.765(4)$ Å, $b = 30.769(6)$ Å, $c = 21.541(5)$ Å, $\beta = 116.01(3)°$), and $[Eu(L^{11})_3](ClO_4)_3 \cdot 4.28MeCN$ (**5a**, monoclinic, $P\bar{1}$, $a = 14.166(3)$ Å, $b = 19.212(4)$ Å, $c = 21.099(4)$ Å, $\alpha = 108.91(3)°$, $\beta = 98.22(3)°$, $\gamma = 108.40(3)°$) have been solved. In **1a**, two different types of complex cations are evidenced, both containing 10-coordinate La(III) ions. In the first type, both perchlorate anions are bidentate, while in the second type, one perchlorate is monodentate, the 10th coordination position being occupied by a water molecule. In **5a** the three ligands are not equivalent. Ligands A and B are wrapped in a helical way and are mirror images of each other, while ligand C lies almost perpendicular to the two other ones. This stems from the steric hindrance generated by the bulky neopentyl groups with the consecutive loss of any stabilizing interstrand π-stacking interactions. This explains the low stability of the tris complexes and the difficulty of isolating them and points to the importance of the steric factors in the design of self-assembled triple helical lanthanide-containing functional edifices $[Ln(L^{i})_3]^{3+}$.

Introduction

The past 2 decades have seen a considerable surge of interest in the coordination chemistry of lanthanide ions, mostly due to applications in biomedical analyses,[1] where lanthanide complexes are used either as diagnostic[2] or as therapeutic[3,4] tools. Both the peculiar magnetic and optical properties of the Ln(III) ions are taken advantage of, for example, in contrast agents for magnetic resonance imaging,[5] in time-resolved fluoroimmunoassays,[6,7] in luminescent specific imaging agents for tissues,[8,9] in luminescent responsive systems to assay various analytes,[10] in the selective hydrolysis of DNA and RNA,[11,12] or in cancer radio- and phototherapy.[4] One real challenge pertaining to the design of functional lanthanide-containing coordination compounds lies, among other features, in the need for a precise control of the Ln(III) inner coordination sphere, while these ions present nondirectional bonding.[13] Several strategies have been developed to master this difficulty, for instance, the encapsulation of the spherical Ln(III) ions into preorganized macrocyclic ligands, into macrocyclic ligands fitted

[†] Institute of Inorganic and Analytical Chemistry, University of Lausanne.
[‡] Institute of Crystallography, University of Lausanne.
[§] University of Geneva.
[||] Hoffmann-La Roche.

(1) Bünzli, J.-C. G.; André, N.; Elhabiri, M.; Muller, G.; Piguet, C. *J. Alloys Compnds.* **2000**, *303/304*, 66−74.
(2) Yam, V. W. W.; Lo, K. K. W. *Coord. Chem. Rev.* **1999**, *184*, 157−240.
(3) Sessler, J. L.; Dow, W. C.; Oconnor, D.; Harriman, A.; Hemmi, G.; Mody, T. D.; Miller, R. A.; Qing, F.; Springs, S.; Woodburn, K.; Young, S. W. *J. Alloys Compnds.* **1997**, *249*, 146−152.
(4) Guo, Z. J.; Sadler, P. J. *Angew. Chem., Int. Ed.* **1999**, *38*, 1513−1531.
(5) Caravan, P.; Ellison, J. J.; McMurry, T. J.; Lauffer, R. B. *Chem. Rev.* **1999**, *99*, 2293−2352.
(6) Mathis, G. In *Rare Earths*; Saez Puche, R., Caro, P., Eds.; Editorial Complutense: Madrid, 1998; pp 285−297.
(7) Hemmilä, I.; Ståhlberg, T.; Mottram, P. *Bioanalytical Applications of Labelling Technologies*; Wallac Oy: Turku, Finland, 1995.
(8) Bornhop, D. J.; Hubbard, D. S.; Houlne, M. P.; Adair, C.; Kiefer, G. E.; Pence, B. C.; Morgan, D. L. *Anal. Chem.* **1999**, *71*, 2607−2615.
(9) Kiefer, G. E.; Jackson, L.; Bornhop, D. J. U.S. Patent 5,928,627, 1999.
(10) Parker, D. *Coord. Chem. Rev.* **2000**, *205*, 109−130.
(11) Komiyama, M.; Takeda, N.; Shigekawa, H. *Chem. Commun.* **1999**, 1443−1451.
(12) Pratviel, G.; Bernardou, J.; Meunier, B. *Adv. Inorg. Chem.* **1998**, *45*, 251.
(13) Bünzli, J.-C. G. In *Rare Earths*; Saez Puche, R., Caro, P., Eds.; Editorial Complutense: Madrid, 1998; pp 223−259.

10.1021/ic001289o CCC: $20.00
Published on Web 05/04/2001

Chart 1

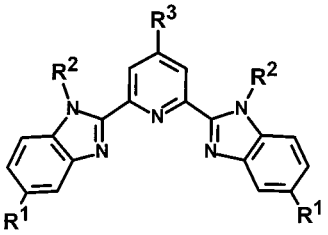

R^1	R^2	R^3	L^i
H	H	H	L^0
H	Me	H	L^1
H	Et	H	L^2
H	$Bz(OMe)_2$	H	L^4
Me	Et	H	L^5
H	$Bz(OMe)_2$	$PhNO_2$	L^7
H	$Bz(Ome)_2$	$PhNEt_2$	L^8
H		H	L^{11}

with dangling arms, or into cavities formed upon self-assembly of carefully tailored multidentate ligands and podands.[14,15] In the latter strategy, judicious design of the ligands leads to weak noncovalent interstrand interactions that stabilize the functional edifices. Working along these lines, we have shown that bis(benzimidazole)pyridines L^i (Chart 1) are versatile tridentate aromatic donors that can be easily derivatized and used as building blocks for various receptors. Monometallic 1:1 nitrato complexes with L^i display photophysical properties that can be tuned by varying the substituents R^1 and R^2 [16,17] and can provide the basis for luminescent liquid crystals.[18,19] In the absence of a strongly coordinating anion, L^i ligands wrap around the Ln(III) ions in a thermodynamically controlled self-assembly process to yield triple helical edifices with electronic and photophysical properties that are controlled by the substituents on the aromatic core.[20−22] Increasing the ligand programming leads to ditopic pentadentate or hexadentate receptors coded for the assembly of d−f[23−25] or f−f[26,27] bimetallic functional helicates.

Triple helical edifices have inherent chirality and may be used as probes for chiral recognition. For instance, the luminescence of racemic $[Ln(dpa)_3]^{3-}$ (Ln = Eu, Tb, H_2dpa = dipicolinic acid) sustains a diastereomeric quenching by ferricytochrome *C* proteins,[28] while enantiopure Δ and Λ cationic lanthanide complexes with a ligand derived from the cyclen framework display stereoselective binding and base-pair selectivity for CT-DNA.[29] Despite the relatively poor luminescent properties of the triple helical $[Ln(L^i)_3]^{3+}$ complexes so far isolated,[30] we have undertaken a study aimed at designing chiro-optical active triple helical complexes with L^i. As a first step toward this goal, we present here the synthesis of ligand L^{11}, fitted with (*S*)-neopentyl N-substituents, and a structural and thermodynamic study of its interaction with trivalent lanthanide ions. We show that the bulky alkyl moiety prevents the wrapping of the third ligand, leading to a peculiar solid-state structure and to very small K_3 stability constants.

Experimental Section

General. Solvents and starting materials were purchased from Fluka AG (Buchs, Switzerland) and used without further purification unless otherwise stated. Acetonitrile was distilled from CaH_2 and P_2O_5. Dichloromethane (CH_2Cl_2), *N*,*N*-dimethylformamide (DMF), and triethylamine were distilled from CaH_2. Lanthanide perchlorates and trifluoromethanesulfonates (triflates) were prepared from the oxides (Rhodia, 99.99%) and dried according to published procedures.[31,32] The Ln content of solutions and solid salts was determined by complexometric titrations with Titriplex III (Merck) in the presence of urotropine and xylene orange.[33] **Caution:** Dry perchlorates and their complexes with aromatic amines may easily explode and should be handled in small quantities and with extreme precaution.[34]

Spectroscopic Measurements. IR spectra were obtained from KBr pellets with a Mattson Alpha Centauri or a Bruker IFS-113v FT spectrometer. Calculations of stability constants from NMR data were performed with the program MINEQL$^+$.[35] UV−vis spectra were recorded using quartz cells of 1.000, 0.100, or 0.010 cm path length (Hellma) on Perkin-Elmer Lambda 7 and 900 spectrometers. Specific rotary dispersion values were measured from 10^{-3} M solution in degassed anhydrous acetonitrile at 298 K with the help of a JASCO DIP-370 polarimeter (sodium D line). ^{1}H and ^{13}C NMR spectra and experiments ({^{1}H−^{1}H} correlation spectroscopy (COSY), {^{1}H−^{13}C} heteronuclear single quantum coherence (HSQC), rotating-frame Overhauser enhancement spectroscopy (ROESY), and distortionless enhancement by polarization transfer (DEPT-135[36])) were performed on Bruker AM-360 (360.15 MHz) and DRX-400 AVANCE (400.03 MHz) spectrometers. Chemical shifts are given in ppm with respect to TMS. Pneumatically assisted electrospray mass spectra were recorded from 10^{-4} M solutions in acetonitrile on an API III tandem mass spectrometer (PE Sciex) by infusion at 4−10 μL min^{-1}. Elemental analyses were carried out by Dr. H. Eder of the Microchemical Laboratory of the University of Geneva.

Preparation of the Ligand L^{11}. The ligand 2,6-bis(benzimidazol-2-yl)pyridine (L^0) was synthesized according to a procedure previously

(14) Piguet, C.; Bünzli, J.-C. G. *Chem. Soc. Rev.* **1999**, *28*, 347−358.
(15) Piguet, C.; Edder, C.; Nozary, H.; Renaud, F.; Rigault, S.; Bünzli, J.-C. G. *J. Alloys Compnds.* **2000**, *303/304*, 94−103.
(16) Piguet, C.; Williams, A. F.; Bernardinelli, G.; Moret, E.; Bünzli, J.-C. G. *Helv. Chim. Acta* **1992**, *75*, 1697−1717.
(17) Petoud, S.; Bünzli, J.-C. G.; Schenk, K. J.; Piguet, C. *Inorg. Chem.* **1997**, *36*, 1345−1353.
(18) Nozary, H.; Piguet, C.; Tissot, P.; Bernardinelli, G.; Bünzli, J.-C. G.; Deschenaux, R.; Guillon, D. *J. Am. Chem. Soc.* **1998**, *120*, 12274−12288.
(19) Nozary, H.; Piguet, C.; Rivera, J.-P.; Tissot, P.; Bernardinelli, G.; Vulliermet, N.; Weber, J.; Bünzli, J.-C. G. *Inorg. Chem.* **2000**, *39*, 5286−5298.
(20) Piguet, C.; Williams, A. F.; Bernardinelli, G.; Bünzli, J.-C. G. *Inorg. Chem.* **1993**, *32*, 4139−4149.
(21) Piguet, C.; Bünzli, J.-C. G.; Bernardinelli, G.; Bochet, C. G.; Froidevaux, P. *J. Chem. Soc., Dalton Trans.* **1995**, 83−97.
(22) Petoud, S.; Bünzli, J.-C. G.; Renaud, F.; Piguet, C.; Schenk, K. J.; Hopfgartner, G. *Inorg. Chem.* **1997**, *36*, 5750−5760.
(23) Edder, C.; Piguet, C.; Bünzli, J.-C. G.; Hopfgartner, G. *J. Chem. Soc., Dalton Trans.* **1997**, 4657−4663.
(24) Piguet, C.; Edder, C.; Rigault, S.; Bernardinelli, G.; Bünzli, J.-C. G.; Hopfgartner, G. *J. Chem. Soc., Dalton Trans.* **2000**, 3999−4006.
(25) Edder, C.; Piguet, C.; Bernardinelli, G.; Mareda, J.; Bochet, C. G.; Bünzli, J.-C. G.; Hopfgartner, G. *Inorg. Chem.* **2000**, *39*, 5059−5073.
(26) Platas, C.; Elhabiri, M.; Hollenstein, M.; Bünzli, J.-C. G.; Piguet, C. *J. Chem. Soc., Dalton Trans.* **2000**, 2031−2043.
(27) Elhabiri, M.; Scopelliti, R.; Bünzli, J.-C. G.; Piguet, C. *J. Am. Chem. Soc.* **1999**, *121*, 10747−10762.
(28) Meskers, S. C. J.; Ubbink, M.; Canters, G. W.; Dekkers, H. P. J. M. *J. Phys. Chem.* **1996**, *100*, 17957−17969.
(29) Govenlock, L. J.; Mathieu, C. E.; Maupin, C. L.; Parker, D.; Riehl, J. P.; Siligardi, G.; Williams, J. A. G. *Chem. Commun.* **1999**, 1699−1700.
(30) Petoud, S.; Bünzli, J.-C. G.; Glanzman, T.; Piguet, C.; Xiang, Q.; Thummel, R. P. *J. Lumin.* **1999**, *82*, 69−79.
(31) Bünzli, J.-C. G.; Mabillard, C. *Inorg. Chem.* **1986**, *25*, 2750−2754.
(32) Bünzli, J.-C. G.; Pilloud, F. *Inorg. Chem.* **1989**, *28*, 2638−2642.
(33) Schwarzenbach, G. *Complexometric Titrations*; Chapman & Hall: London, 1957; p 8 ff.
(34) Wolsey, W. C. *J. Chem. Educ.* **1973**, *50*, A335−A337.
(35) Schecher, W. *MINEQL$^+$*, version 2.1; MD Environmental Research Software: Edgwater, NJ, 1991.
(36) Popov, A.; Hallenga, K. *Modern NMR Techniques and Their Applications in Chemistry*; *Practical Spectroscopy Series* 11; M. Dekker: New York, 1991.

Table 1. Crystallographic Data for L^{11}, **1a**, and **5a**

	L^{11}	**1a**	**5a**
formula	$C_{29}H_{33}N_5$	$C_{262}H_{311}Cl_{12}La_4N_{55}O_{49}$	$C_{95.58}H_{111.84}N_{19.28}O_{12}Cl_3Eu$
fw	451.61	6052.92	1982.29
space group	$P2_1$	$P2_1$	$P\bar{1}$
a, Å	13.4850(12)	21.765(4)	14.166(3)
b, Å	12.0243(11)	30.769(6)	19.212(4)
c, Å	16.4239(14)	21.541(5)	21.099(4)
α, deg	90	90	108.91(3)
β, deg	103.747(7)	116.01(3)	98.22(3)
γ, deg	90	90	108.40(3)
V, Å^3	2586.8(4)	14169(5)	4958(2)
Z	4	2	2
T, °C	20	−103	−103
λ, Å	0.710 73	0.710 73	0.710 73
D_{calcd}, g cm^3	1.160	1.405	1.328
$\mu_{Mo\ K\alpha}$, mm^{-1}	0.70	0.785	0.781
R1[a]	0.0400	0.0698	0.0772
wR2[b]	0.0980	0.1013	0.1955

[a] $R = \sum[|F_o| - |F_c|]/\sum|F_o|$. [b] $R_w(F_o^2) = [\sum w(F_o^2 - F_c^2)^2/\sum w(F_o^4)]^{1/2}$.

described.[37] Ligand L^{11} was prepared under N_2. A total of 238 mg of L^0 (0.74 mmol) was dissolved in 10 mL of dry THF. The mixture was cooled to 0 °C, then a total of 178 mg of KH (4.44 mmol) previously washed with 5 × 10 mL of dry pentane was added. The mixture was allowed to stand at room temperature, stirred for 60 min before the addition of 1.17 g of 18-crown-6 (4.44 mmol) in dry THF and 550 *μ*L of *S*(+)-1-bromo-2-methylbutane (4.44 mmol). The solution was put into an autoclave and refluxed for 3 days. The KBr was filtered off, and the resulting mixture was poured into water (100 mL). Then an amount of 50 mL of THF was added. The organic layer was separated, and the aqueous phase was extracted with $CHCl_3$ (3 × 100 mL). The combined organic phases were dried over Na_2SO_4 and evaporated. The resulting crude solid was purified by column chromatography (Al_2O_3, CH_2Cl_2) and recrystallized by slow diffusion of hexane into a dichloromethane solution to give 200 mg of L^{11} (0.44 mmol, 58%). Mp, 100−102 °C. ^{1}H NMR in $CDCl_3$: *δ* 0.63 (6H, d, ^3J = 7 Hz), 0.66 (6H, t, ^3J = 7.2 Hz), 0.97 (2H, m, ^3J = 7.1 Hz, ^2J = 14.2 Hz), 1.18 (2H, m, ^3J = 7.1 Hz, ^2J = 14.2 Hz), 1.87 (2H, pseudo-octet, ^3J = 6−8 Hz), 4.56 (2H, dd, ^3J = 7.9 Hz, ^2J = 14.1 Hz), 4.69 (2H, dd, ^3J = 7.1 Hz, ^2J = 14.1 Hz), 7.33−7.48 (6H, m), 7.88 (2H, m), 8.05 (1H, t, ^3J = 7.9 Hz), 8.33 (2H, d, ^3J = 7.9 Hz). ^{13}C NMR in $CDCl_3$: *δ* 9.96 (2C), 15.80 (2C), 26.21 (2C), 35.42 (2C), 50.10 (2C), 110.99 (2C), 119.30 (2C), 122.14 (2C), 123.04 (2C), 124.84 (2C), 136.67 (1C), 138.02, 142.29, 149.85, 150.08 (8 C_{quat}). With respect to L^0, IR data show the disappearance of the NH vibration. Electrospray mass spectrometry (ES-MS) (MeCN): *m*/*z* 452.2 ([L + H]$^+$).

Preparation of the Complexes. The 1:2 complexes $[Ln(ClO_4)_2(L^{11})_2](ClO_4)$ and $[Eu(CF_3SO_3)_2(L^{11})_2](CF_3SO_3)$ were prepared by mixing L^{11} with stoichiometric amounts of $Ln(ClO_4)_3 \cdot nH_2O$ (Ln = La, Eu, Tb; *n* = 0.2−0.6) in dichloromethane-acetonitrile. The complexes may be crystallized in 70−80% yield by slow diffusion of *tert*-butyl methyl ether into an acetonitrile solution. The $[Eu(L^{11})_3](ClO_4)_3$ complex was prepared in 20−30% yield according to the same procedure, using a large excess of ligand (Eu/L = 1:6).

The ligand L^{11} and each of the complexes were characterized by their IR spectra and gave satisfactory elemental analyses (Table T1 of Supporting Information).

Spectrophotometric Titrations. Electronic spectra in the UV−visible range were recorded at 298 K from 10^{-4} mol dm^{-3} acetonitrile solutions containing 0.1 M Et_4NClO_4 as an inert electrolyte with a Perkin-Elmer Lambda 7 spectrometer connected to an external computer and using quartz cells of 0.100 cm path length. Solutions were prepared in a thermostated vessel (Metrohm 6.1418.220), and the titrant solution was added with an automated buret from Metrohm (6.1569.150 or 6.1569.210) fitted with a antidiffusion device. In a typical experiment, 5−10 mL of L^{11} were titrated with a solution of Ln(III) triflate 10^{-4} M in acetonitrile. After each addition of 0.20 mL and a delay of 2 min, the spectrum was measured and transferred to the computer. In some instances, reverse titrations, i.e. with L^{11} as titrating species, were also performed to confirm the values of the stability constants. All the experiments were conducted in a drybox, and the water content of the solutions, measured at the end of the titration by the Karl Fischer method, was always <30 ppm. Factor analysis and stability constant determinations were carried out with the program SPECFIT, version 2.10.[38]

X-ray Experimental Section. 1. L^{11}. A thin bent crystal without any well-defined habitus was glued on a glass needle and exposed to graphite monochromatized Mo Kα radiation. The data were collected on a KUMA diffractometer equipped with a CCD detector and a four-circle *κ*-goniometer (Table 1). A little more than one hemisphere of reflections were collected. Newly developed algorithms and programs[39−41] were used in the data reduction. Data were corrected for Lorentz and polarization effects but not for absorption. The structure was solved using direct methods.[42] All C and N atoms were refined anisotropically. Hydrogen atoms were clearly visible in difference maps and were generated using a riding atom model. The structure is pseudocentrosymmetric, the atoms not fitting the higher symmetry being found in the side chains. This renders refinement of the absolute structure impossible, but the structure is otherwise refinable in the noncentrosymmetric space group. The proposed chirality is the one corresponding to a postrefinement Flack parameter[41] around zero. The chirality centers C23 and C31 are *S* for both molecules, as expected from the synthesis.

2. $[La(ClO_4)_2(L^{11})_2]_3[La(ClO_4)_2(H_2O)(L^{11})_2](ClO_4)_4 \cdot 15MeCN$ (1a). The pale-pinkish, lathlike crystals were directly transferred from their mother liquor into a drop of Hostinert 216 and kept at 210 K. A specimen was selected, cut to size, and finally placed in a glass capillary. The data collection, at 170 K, took place on a Stoe IPDS system equipped with Mo Kα radiation (Table 1). The image plate−crystal distance was set to 80 mm, and a *φ* interval of 1° was chosen. Two hundred images were exposed for 4 min each. An inspection of reciprocal space revealed the diffraction figure to consist essentially of maxima (∼90%) indexable in the cell of Table 1 (the remaining weak peaks were due to powdery features or sheer noise). These were integrated using profiles between 13 and 19 pixels and a mosaic spread of 0.007. The intensities were corrected for Lorentz and polarization effects. The absorption correction used Gaussian integration and yielded transmission factors between 0.699 13 and 0.914 22. The decay during the measurement was negligible. The structure was solved with the

(37) Addison, A. W.; Burke, P. J. *J. Heterocycl. Chem.* **1981**, *18*, 803−805.
(38) Gampp, H.; Maeder, M.; Meyer, C. J.; Zuberbühler, A. D. *Talanta* **1986**, *33*, 943−951.
(39) Paciorek, W. A.; Meyer, M.; Chapuis, G. *J. Appl. Crystallogr.* **1999**, *32*, 11−14.
(40) Paciorek, W. A.; Meyer, M.; Chapuis, G. *Acta Crystallogr., Sect. A: Fundam. Crystallogr.* **1999**, *55*, 543−557.
(41) Flack, H. D. *Acta Crystallogr.* **1983**, *A39*, 876−881.
(42) Sheldrick, G. M. *Acta Crystallogr.* **1997**, *A46*, 467−473.

Scheme 1

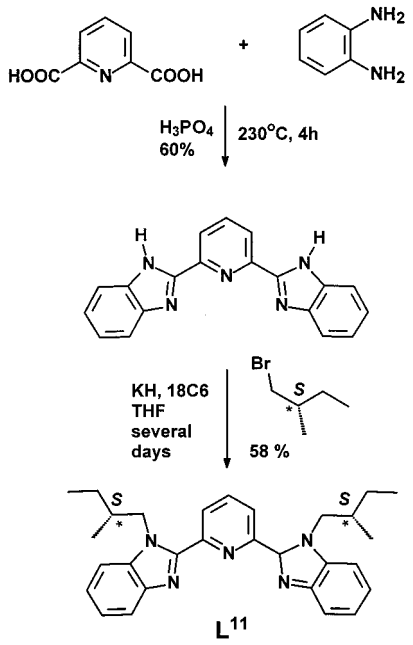

help of SHELXTL 5.05,[43] in space group $P2_1$, and some corollary calculations were carried out by means of PLATON.[44] Rigid links had to be imposed on some atoms during refinement. The acetonitrile molecules could only be refined under geometrical restraints.

3. $[Eu(L^{11})_3](ClO_4)_3 \cdot 4.28MeCN$ (5a). The pale-pinkish, lathlike crystals were directly transferred from their mother liquor into a drop of Hostinert 216 kept at 210 K. A specimen was selected, cut to size, and placed in a glass capillary. The data collection at 170 K took place on a Stoe IPDS system equipped with Mo Kα radiation (Table 1). The image plate−crystal distance was set to 80 mm, and a ϕ interval of 1° was chosen. Two hundred images were then exposed for 4 min each. An inspection of reciprocal space revealed the crystals to be pseudo-merohedric twins. The dominant individuum accounted for two-thirds of the peaks, and for the remaining ones another orientation matrix could be found. The integration (based on an effective mosaic spread of 0.004) was carried out by using the dominant orientation matrix but keeping track of the second one as well. A peak overlap of two pixels was tolerated in order to retain the maximum number of reflections. Nevertheless, almost half of the reflections were eliminated because of severe peak overlap. The intensities were corrected for Lorentz and polarization effects but not for absorption because the crystal was invisible in the frozen oil (the absorption coefficient appears to be negligible; cf. Table 1). The decay during measurement was insignificant. The structure was solved in space group $P\bar{1}$ with the help of SHELXTL 5.05,[43] using all reflections of the dominant individuum; corollary calculations were carried out by means of PLATON.[44] Most of the butane sidearms of the ligand were disordered, and restraints had to be applied. More precisely, standard distances were imposed between first and second neighboring carbon atoms of the sidearms, and the population parameters of the two terminal carbon atoms were allowed to vary, their sum being restrained to 1.

Results

Ligand Synthesis and Characterization. Ligand L^{11} was synthesized through N-alkylation of 2,6-bis(benzimidazol-2-yl)-pyridine according to a procedure similar to those reported for the syntheses of L^1 and L^2 (Scheme 1).[21] The reaction rate is rather slow, so in order to obtain a reasonable yield (58%), the alkylation was performed in a pressurized vessel for several days and in the presence of 18-crown-6 to complex potassium ions. The absolute configuration of the asymmetric carbon atoms of the neopentyl arms is retained, as demonstrated by the value of the specific optical rotation: $[\alpha]_D^{25} = 15.1 \pm 0.3$ deg dm^2 mol^{-1}.

Chart 2

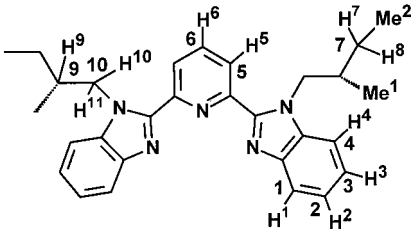

Table 2. Species Observed in the ES-MS Spectra of 10^{-3} M Solutions in Acetonitrile with $[L^{11}]_t/[Eu^{3+}]_t = 1$, 2, and 3 at 298 K

species	m/z[a]	species	m/z[a]
$[Eu(MeCN)_3(L^{11})]^{3+}$	242.4	$[Eu(ClO_4)(MeCN)_3(L^{11})]^{2+}$	413.2
$[Eu(MeCN)_4(L^{11})]^{3+}$	256.1	$[Eu(ClO_4)(MeCN)_4(L^{11})]^{2+}$	433.3
$[Eu(MeCN)_5(L^{11})]^{3+}$	269.8	$[(L^{11}) + H]^+$	452.3
$[Eu(L^{11})_2]^{3+}$	351.9	$[Eu(L^{11})_3]^{3+}$	502.3
$[Eu(MeCN)(L^{11})_2]^{3+}$	365.5	$[Eu(ClO_4)(L^{11})_2]^{2+}$	577.2
$[Eu(ClO_4)(MeCN)(L^{11})]^{2+}$	371.7	$[Eu(ClO_4)(MeCN)(L^{11})_2]^{2+}$	597.6
$[Eu(MeCN)_2(L^{11})_2]^{3+}$	379.3	$[Eu(ClO_4)(L^{11})_3]^{2+}$	802.9
$[Eu(MeCN)_2(L^{11})_2(H_2O)]^{3+}$	385.2	$[2(L^{11}) + H]^+$	903.6
$[Eu(ClO_4)(MeCN)_2(L^{11})]^{2+}$	392.6	$[Eu(ClO_4)(L^{11})_4]^{2+}$	1028.5

[a] m/z values given for the maximum of the peak at unit mass resolution.

With respect to L^0, IR data show the disappearance of the NH vibration, while aromatic C=C modes occur at 1568 and 1590 cm^{-1}. ^{1}H (11 resonances) and ^{13}C (13 resonances) NMR spectra in CD_3CN (5×10^{-3} M) are consistent with the presence of a single species with a bis(benzimidazole)pyridine core having C_2 symmetry (Figure F1 of Supporting Information). For instance, a singlet and a doublet ($^3J = 7.9$ Hz) are observed for C^5 and H^5, respectively (Chart 2). The pyridine protons H^5 and H^6 display pseudo-first-order spectra, while the benzimidazole protons H^1-H^4 give rise to a complicated ABCD spectrum. The aliphatic region contains one doublet and one triplet assigned to Me^1 and Me^2, while the geminal pairs $H^{7,8}$ and $H^{10,11}$ are not equivalent, generating two closely spaced multiplets in the ranges 0.92−1.22 and 4.50−4.80 ppm, respectively. The signal from proton H^9 is a pseudo-octuplet, reflecting couplings to Me^1, $H^{7,8}$, and $H^{10,11}$. As observed for the other L^i ligands,[22] the conformation of the molecule is trans−trans, a nuclear Overhauser effect being observed between H^4 and H^{10} (or H^{11}) while none exists between H^5 and H^{10} (or H^{11}). This conformation also prevails in the solid state, as demonstrated by the X-ray crystal structure (Table 1, Figure 1). The unit cell contains two independent molecules A and B, the bond lengths and angles of which differ only slightly (Table T2 of Supporting Information). All aromatic groups are planar, but the benzimidazole moieties are not coplanar with the pyridine, the interplanar angles being very similar and in the range 23.4−27.2° (Table T3 of Supporting Information). Two largely different interplanar angles have been reported for $[HL^1]^+$ (30.5° and 45.3° [17]) and L^7 (12.8° and 41.8° [45]) and have been attributed to a minimization of the steric repulsion of the arms. In L^{11}, the two arms lie on both sides of the pyridine ring, so steric constraints are minimal, henceforth resulting in two relatively small and equal interplanar angles. The crystal packing is

(43) Sheldrick, G. M. *SHELXTL*, version 5.05; Siemens Analytical X-Ray Instruments, Inc.: Madison, WI, 1996.
(44) Speek, A. L. *Acta Crystallogr.* **1990**, *A46*, C34.
(45) Petoud, S. Ph.D. Dissertation, University of Lausanne, Lausanne, Switzerland, 1997.

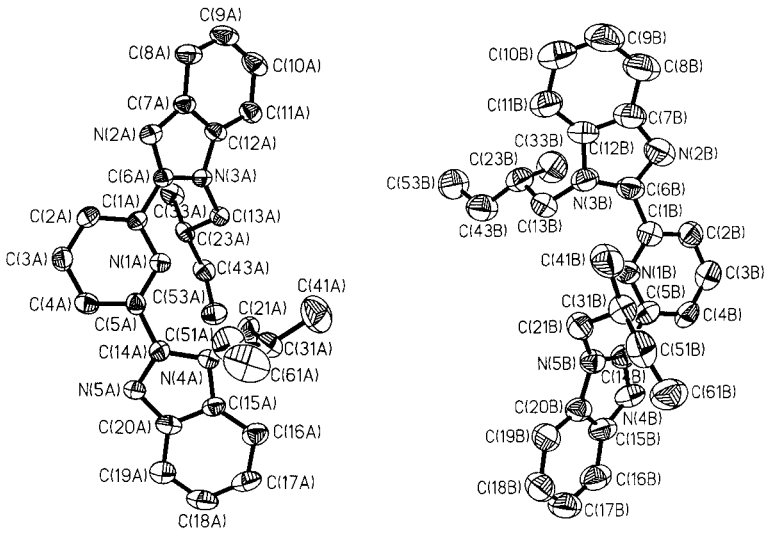

Figure 1. Molecular structure and numbering scheme for the two types of L^{11} molecules found in the unit cell.

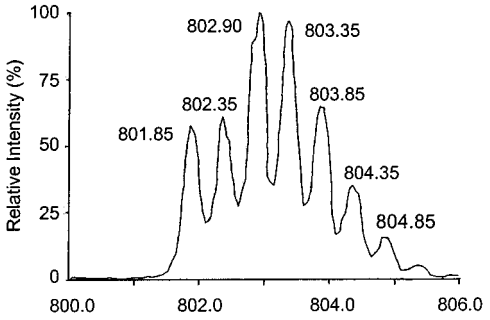

Figure 2. Detail of the ES-MS signal arising from the $[Eu(L^{11})_3(ClO_4)]^{2+}$ species ($[Eu]_t = 10^{-4}$ M in anhydrous acetonitrile).

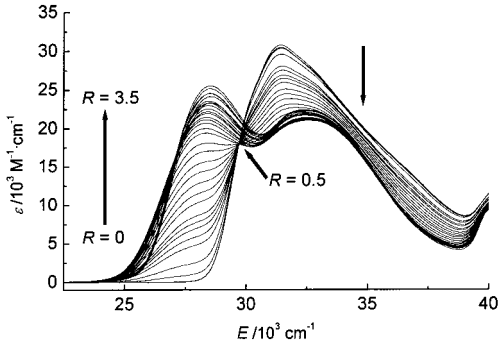

Figure 3. Absorption spectra (corrected for dilution) obtained while titrating 4.3×10^{-4} M L^{11} with 1.5×10^{-3} M $Eu(Otf)_3$ in CH_3CN. $R = [Eu]_t/[L^{11}]_t$.

dominated by weak π-stacking interactions between parallel benzimidazole rings from two different molecules (A and B), with interplanar distances in the range 3.56−3.76 Å (Figure F2 of Supporting Information).

Interaction Between L^{11} and Ln(III) Ions. Electrospray mass spectra have been measured for solutions with Eu(III)-to-L^{11} ratios R equal to 1, 0.5, and 0.33 in the concentration range 10^{-3}−10^{-4} M to establish the speciation in acetonitrile (Table 2 and Figure F3 of Supporting Information). Perchlorate adducts and isotopic distribution help in identifying the species, as shown in Figure 2. The main signals observed for solutions with $R = 1$ are assigned to the $[Eu(ClO_4)_x(L^{11})(MeCN)_y]^{(3-x)+}$ species, with, in addition, weak signals from 1:2 species. The most intense signals in the spectra of solutions with $R = 0.5$ are assigned to the $[Eu(ClO_4)_x(L^{11})_2(MeCN)_y]^{(3-x)+}$ species, while smaller signals from 1:1 and 1:3 species are also present. Peaks from the latter species become important in the solutions with $R = 0.33$, but signals from the 1:1 and 1:2 complexes are still present (Figure F3 of Supporting Information). From these data, one can infer the successive formation of the 1:1, 1:2, and 1:3 complexes, although the last does not appear to form quantitatively. In ES-MS experiments with lanthanide complexes, the more solvated a species is, the more difficult it is to transfer it to the gas phase, so the signal intensities cannot be used to assess the relative quantity of the observed complexes and adducts.[46]

To quantify the Ln(III)−L^{11} interaction, we have performed spectrophotometric titrations of L^{11} by $Ln(Otf)_3$ (Ln = La, Eu, Lu) at 298 K in the presence of 0.1 M Et_4NClO_4 under anhydrous conditions ($[H_2O]$ < 30 ppm). Factor analysis indicates the presence of three or four absorbing species, and the data (Figure 3) have been fitted by a least-squares procedure using either equilibrium reactions 1 and 2 or equilibrium reactions 1−3, where solvation and anion coordination has been omitted:

$$Ln^{3+} + L^{11} \rightleftharpoons [Ln(L^{11})]^{3+} \qquad \log K_1 \qquad (1)$$

$$[Ln(L^{11})]^{3+} + L^{11} \rightleftharpoons [Ln(L^{11})_2]^{3+} \qquad \log K_2 \qquad (2)$$

$$[Ln(L^{11})_2]^{3+} + L^{11} \rightleftharpoons [Ln(L^{11})_3]^{3+} \qquad \log K_3 \qquad (3)$$

Electronic spectra of the three complex species are correlated, which renders the fitting process difficult and results in relatively large uncertainties on $\log K_i$ values. Both models lead to $\log K_1$ and $\log K_2$ values that are in reasonable agreement (Table 4). When all reactions 1−3 are used, the residuals are smaller; however, the three stability constants could not be calculated simultaneously in the case of La(III) and Eu(III) and one or two of them had to be fixed in order to extract the other one(s). This prompted us to check whether these values are consistent with ^1H NMR data.

Figure 4 presents the spectra obtained with La(III). Signals from the 1:1 and 1:2 complexes could be clearly identified for La(III), Eu(III), and Lu(III) (Table 3), while only two broad signals arising from the aromatic protons $H^{5,6}$ of the Eu(III) 1:3 species could be assigned unambiguously in a solution

(46) Stewart, I. I.; Horlick, G. *Anal. Chem.* **1994**, *66*, 3983−3993.

Table 3. ^{1}H NMR Shifts Observed for L^{11} and for Its 1:1, 1:2, and 1:3 Complexes with Ln(III) Ions (CD_3CN, 5×10^{-3} M, 298 K)

species	H^1	H^2	H^3	H^4	H^5	H^6	$H^{7,8}$	H^9	$H^{10,11}$	Me^1	Me^2
L^{11}	7.76	7.28−7.37	7.28−7.37	7.59	8.29	8.11	0.96, 1.14	1.83	4.54, 4.77	0.57	0.60
La 1:1	8.41	7.50	7.55	7.78	8.37	8.47	1.19, 1.39	2.02	4.54, 4.68	0.79	0.85
La 1:2	7.64	7.27	6.91	7.23	8.49	8.42	1.24, 1.43	2.03	4.53, 4.68	0.82	0.89
Eu 1:1	8.36	5.65	6.49	4.52	4.62	7.15	0.75	0.96	3.08, 3.32	0.35	0.69
Eu 1:2	8.32	5.66	6.27	4.51	9.36	11.09	1.00	1.61	3.62, 3.86	0.37	0.83
Eu 1:6[a]	*b*	*b*	*b*	*b*	8.68	10.59	*b*	*b*	*b*	*b*	*b*
Lu 1:1	8.24	7.84	7.58	6.98	8.45	8.56	1.33, 1.48	2.11	4.61, 4.70	0.92	0.93
Lu 1:2	8.32	7.58	7.26	6.97	8.65	8.82	0.77, 1.31	2.11	4.53, 4.67	0.64	0.94

[a] From a solution with a ratio Eu(III)/L^{11} = 1:6. [b] Too weak to be identified.

Table 4. Stability Constants of $[Ln(L^{11})_n]^{3+}$ Complexes (n = 1−3) As Determined by NMR and UV−Vis Spectrometry (μ = 0.1 M Et_4NClO_4, 298 K)

	log K_1			log K_2			log K_3	
Ln	UV−vis[a]	UV−vis[b]	NMR	UV−vis[a]	UV−vis[b]	NMR	UV−vis[b]	NMR
La	7.9 ± 0.2	8.0 ±0.3[c]	8.1 ± 0.1	4.9 ± 0.2	6.0 ± 0.4[c]	5.7 ±0.5	5.3 ± 0.6	1.2 ± 0.2
Eu	7.0 ± 0.3	8.2 ± 0.2	8.2 ± 0.2	5.8 ± 0.4	5.9 ± 0.3[d]	5.9 ± 0.3	4.0 ± 0.5	0.9 ± 0.1
Lu	6.9 ± 0.3	8.0 ± 0.2	6.9 ± 0.1	5.7 ± 0.4	6.1 ± 0.3	5.7 ± 0.1	4.3 ± 0.5	*e*

[a] Model with three absorbing species. [b] Model with four absorbing species. [c] Values of log K_1 and log K_2 were fixed (see text). [d] The value of log K_2 was fixed (see text). [e] Not determined. The 1:3 species was not seen in the NMR spectra.

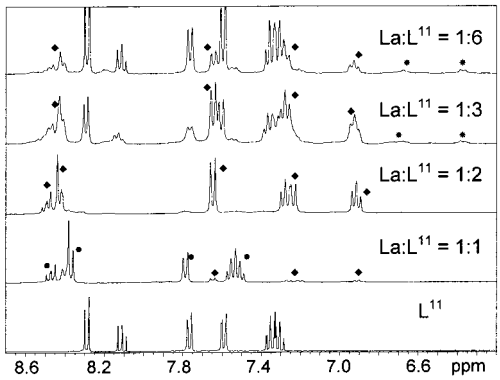

Figure 4. ^{1}H NMR spectra of L^{11} and of solutions containing various ratios of $La(ClO_4)_3 \cdot 0.3H_2O$ (5×10^{-3} M) and L^{11} in anhydrous CD_3CN at 295 K. The symbols ●, ◆, and ∗ denote signals arising from the 1:1, 1:2, and 1:3 species, respectively.

containing an excess of ligand. In the solutions with a stoichiometric ratio R = 0.33, the major species is always the 1:2 complex and is still present in solutions with a large excess of ligand (Ln/L = 1:6), pointing to rather low values of log K_3. Only one series of relatively sharp signals is observed in the NMR spectra of the $[Ln(L^{11})_2]^{3+}$ complexes, consistent with the two ligands being equivalent and with slow ligand exchange processes between free and coordinated ligands on the NMR time scale. The specific optical rotation determined for Ln = La, Eu, and Tb amounts to 35.2 ± 0.3, 33.9 ± 0.4, and 34.4 ± 0.1 deg dm^2 mol^{-1}, respectively, that is marginally larger than twice the value found for the free ligand. Although small, the structural contribution (4−5 deg dm^2 mol^{-1}) to the chiro-optical effect points to a chiral environment of the metal ion.

Integration of several aliphatic and aromatic resonances allowed us to determine the relative concentrations of the species in equilibrium. For La(III), the solution with R = 1 contains 2% free ligand, while 87% and 11% of the ligands are complexed in the 1:1 and 1:2 species, respectively. In the solution with R = 0.5 all ligands are complexed; 9% of the ligands are in the 1:1 species and 91% in the 1:2 species. When R reaches 0.33, free ligand (27%) is again seen, which means that the 1:3 species forms only in small quantities (corresponding to 8% of the ligands), the 1:2 species being the major complex in solution and corresponding to 65% of the ligands. Addition of more ligand (R = 0.167) only slightly increases the proportion of the 1:3 species. For Eu(III), the situation is similar except that the 1:3 species only appears in the spectrum with R = 0.167 while it is not seen at all for Lu(III). The stability constants extracted from ^{1}H NMR data analyzed with MINEQL^{+} [35] are reported in Table 4. Values for log K_1 and log K_2 are in excellent agreement with those obtained by fitting the spectrophotometric data with the model with four absorbing species, except for log K_1(Lu) for which a difference of 1.1 ± 0.3 is observed. A large discrepancy, however, is seen for the log K_3 values determined by the two different techniques, which will be discussed later.

Isolation and Structure of the 1:2 and 1:3 Complexes. When starting from a lanthanide salt with a weakly coordinating anion such as perchlorate or triflate, hygroscopic 1:2 and 1:3 complexes are isolated while the syntheses of the 1:1 complexes require the presence of a strongly coordinating anion such as nitrate, as observed for the other L^i ligands[17] (properties of the nitrato complexes will be presented elsewhere). The following complexes yielded good elemental analysis results (Table T1 of Supporting Information): $[La(ClO_4)_2(L^{11})_2](ClO_4) \cdot 0.5Me_3COMe$ (**1**), $[Eu(ClO_4)_2(L^{11})_2](ClO_4) \cdot 2H_2O$ (**2**), $[Eu(CF_3SO_3)_2(L^{11})_2](CF_3SO_3)$ (**3**), $[Tb(ClO_4)_2(L^{11})_2](ClO_4) \cdot 1.5H_2O$ (**4**), and $[Eu(L^{11})_3](ClO_4)_3 \cdot H_2O$ (**5**). The solvation is difficult to control and depends on the drying conditions. The 1:3 complex is particularly difficult to isolate, even in the presence of a large excess of ligand because the 1:2 species is more stable and less soluble and therefore crystallizes more easily than the 1:3 adduct. Upon complexation, changes in vibrational spectra are evident; in particular, the two C═C ring vibrations of the pyridine and benzimidazole moieties (1590 and 1568 cm^{-1} in the free ligand) are blue-shifted in the complexes by 11−13 and 3−5 cm^{-1} in both 1:2 and 1:3 complexes, respectively. Vibrations for ionic perchlorate only could be identified in the spectrum of the 1:3 complex, while spectra of the 1:2 complexes reveal, in addition, the vibrational modes of monodentate perchlorate (623, 656−659, 924−929, 1025−1027, 1142−1143 cm^{-1}) and some modes that can be attributed to bidentate perchlorate (610−615, 637, and 904−912 cm^{-1}).[47] The $\delta(SO_3)$ mode of the triflate anion

(47) Bünzli, J.-C. G.; Milicic-Tang, A. In *Handbook on the Physics and Chemistry of Rare Earths*; Gschneidner, K. A., Jr., Eyring, L., Eds.; Elsevier Science Publishers B.V.: Amsterdam, 1995; Chapter 145, pp 306−366.

Table 5. Bond Distances (Å) and Angles (deg) in the Coordination Polyhedra of the Complex Cations $[La(ClO_4)_2(L^{11})_2]^+$ (La1−La3) and $[La(ClO_4)_2(L^{11})_2(H_2O)]^+$ (La4)

Bond Distances							
La1−N1A	2.74(1)	La2−N1C	2.79(1)	La3−N1E	2.75(1)	La4−N1G	2.71(1)
La1−N2A	2.64(1)	La2−N2C	2.67(1)	La3−N2E	2.70(1)	La4−N2G	2.65(1)
La1−N5A	2.67(1)	La2−N5C	2.65(1)	La3−N5E	2.71(1)	La4−N5G	2.63(1)
La1−N1B	2.76(1)	La2−N1D	2.74(1)	La3−N1F	2.77 (1)	La4−N1H	2.76(1)
La1−N2B	2.61(1)	La2−N2D	2.63(1)	La3−N2F	2.68(1)	La4−N2H	2.66(1)
La1−N5B	2.64(1)	La2−N5D	2.62(0)	La3−N5F	2.69(1)	La4−N5H	2.64(1)
La1−O11	2.667(1)	La2−O31	2.629(1)	La3−O53	2.585(1)	La4−O72	2.671(1)
La1−O12	2.669(1)	La2−O32	2.648(1)	La3−O555	2.654(1)	La4−O73	2.693(1)
La1−O21	2.679(1)	La2−O41	2.684(1)	La3−O61	2.695(1)	La4−O81	2.639(1)
La1−O22	2.688(1)	La2−O42	2.682(1)	La3−O62	2.676(1)	La4−O82	2.614(1)
Bond Angles							
N1A−La1−N2A	62.7(3)	N1C−La2−N2C	61.2(3)	N1E−La3−N2E	62.3(3)	N1G−La4−N2G	61.8(3)
N1A−La1−N5A	60.8(3)	N1C−La2−N5C	59.8(2)	N1E−La3−N5E	60.4(3)	N1G−La4−N5G	61.5(3)
N1A−La1−N1B	175.6(3)	N1C−La2−N1D	177.2(2)	N1E−La3−N1F	172.3(3)	N1G−La4−N1H	175.1(3)
N1A−La1−N2B	123.4(3)	N1C−La2−N2D	115.0(2)	N1E−La3−N2F	121.7(4)	N1G−La4−N2H	119.9(3)
N1A−La1−N5B	114.5(3)	N1C−La2−N5D	122.2(2)	N1E−La3−N5F	115.3(3)	N1G−La4−N5H	116.9(3)
N2A−La1−N5A	123.4(3)	N2C−La2−N5C	121.1(3)	N2E−La3−N5E	122.7(3)	N2G−La4−N5G	123.2(3)
N2A−La1−N1B	115.3(3)	N2C−La2−N1D	119.2(3)	N2E−La3−N1F	119.8(2)	N2G−La4−N1H	113.6(3)
N2A−La1−N2B	137.8(3)	N2C−La2−N2D	139.4(3)	N2E−La3−N2F	140.4(2)	N2G−La4−N2H	139.2(3)
N2A−La1−N5B	71.2(3)	N2C−La2−N5D	74.7(4)	N2E−La3−N5F	73.2(2)	N2G−La4−N5H	71.8(3)
N5A−La1−N1B	121.2(3)	N5C−La2−N1D	119.7(3)	N5E−La3−N1F	117.2(2)	N5G−La4−N1H	123.2(3)
N5A−La1−N2B	75.7(3)	N5C−La2−N2D	73.0(3)	N5E−La3−N2F	74.1(4)	N5G−La4−N2H	74.6(3)
N5A−La1−N5B	138.3(3)	N5C−La2−N5D	136.9(3)	N5E−La3−N5F	135.2(3)	N5G−La4−N5H	136.5(2)
N1B−La1−N2B	60.8(3)	N1D−La2−N2D	63.1(3)	N1F−La3−N2F	62.1(4)	N1H−La4−N2H	62.1(2)
N1B−La1−N5B	61.2(3)	N1D−La2−N5D	60.3(3)	N1F−La3−N5F	60.5(4)	N1H−La4−N5H	61.1(2)
N2B−La1−N5B	122.1(3)	N2D−La2−N5D	123.3(4)	N2F−La3−N5F	122.6(4)	N2H−La4−N5H	123.0(2)

in **3**, which appears around 635 cm^{-1}, is split, suggesting the presence of both coordinated and ionic triflate.

Slow diffusion of *tert*-butyl methyl ether into a solution of **1** in acetonitrile allowed us to isolate monoclinic crystals suitable for X-ray diffraction, which turned out to have the following formula: $[La(ClO_4)_2(L^{11})_2]_3[La(ClO_4)_2(H_2O)(L^{11})_2](ClO_4)_4 \cdot 15MeCN$ (**1a**). The unit cell belongs to the monoclinic system group and contains two different types of bis(perchlorato) complex cations in the ratio 3:1. These cations are depicted in Figures 5 and F4 (Supporting Information), while bond distances and angles for the La(III) coordination polyhedra are reported in Table 5. A coordination number of 10 prevails for all the La(III) ions. In the first type of complex cation, this number is achieved through the binding of two tridentate ligands and two bidentate perchlorate anions, while in the second type of complex cation, one water molecule displaces one oxygen atom of a perchlorate, resulting in the presence of two anions with different denticity. The two ligands are wrapped around the metal ion in a helical way, as was observed for $[Yb(OH)(L^1)_2]_2^{4+}$ [22] and $[Lu(L^1)_2(MeOH)(H_2O)]^{3+}$.[20] The asymmetric carbon atoms retain their absolute configuration *S* in all the complex cations. Bond distances in the coordinated ligand molecules are close to those observed in uncomplexed L^{11}, but several interplanar angles are modified (Table T4 of Supporting Information). In general, the interplanar angles between the planar pyridine and the two planar benzimidazole moieties lie within a close range for one given coordinated L^{11} molecule, the largest difference amounting to 5.4°, but the interplanar angles in both complex cations are quite different for the two ligands, on average 31° for one molecule and 21° for the other one. A large difference is consequently also observed in the interplanar angles between the benzimidazole groups: on average 26° for one coordinated molecule and 11° for the other. The crystal packing is determined by the presence of several weak intermolecular CH···O H-bonds, each O atom of the noncoordinated perchlorates being involved in two such interactions with H atoms from the neopentyl groups, from the pyridine rings and from acetonitrile. Each noncoordinated anion holds together two $[La(ClO_4)_2(L^{11})_2]^+$ cations and two MeCN molecules (Figure 6, Table T5 of Supporting Information).

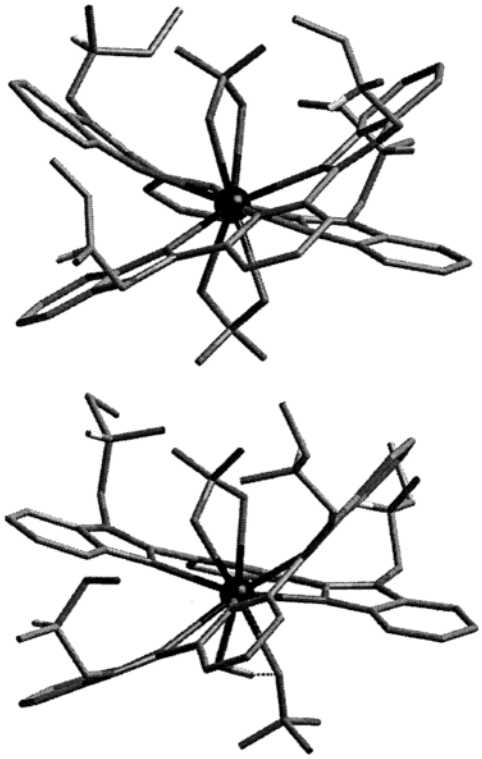

Figure 5. Complex cations $[La(ClO_4)_2(L^{11})_2]^+$ (top) and $[La(ClO_4)_2(L^{11})_2(H_2O)]^+$ (bottom).

Suitable crystals of the Eu(III) 1:3 complex could also be isolated, which turned out to have the following formulation: $[Eu(L^{11})_3](ClO_4)_3 \cdot 4.28MeCN$ (**5a**). The unit cell contains isolated $[Eu(L^{11})_3]^{3+}$cations, noncoordinated perchlorate anions, and heavily disordered acetonitrile molecules, which explains the fractional value found. The structure is featured in Figures 7 and F5 (Supporting Information), selected bond lengths and angles are given in Table 6, while interplanar angles are reported in Table T6 of Supporting Information. Two of the ligand molecules (A and B) are wrapped around the Eu(III) ion in a helical fashion, much as they were in the La(III) 1:2 complex,

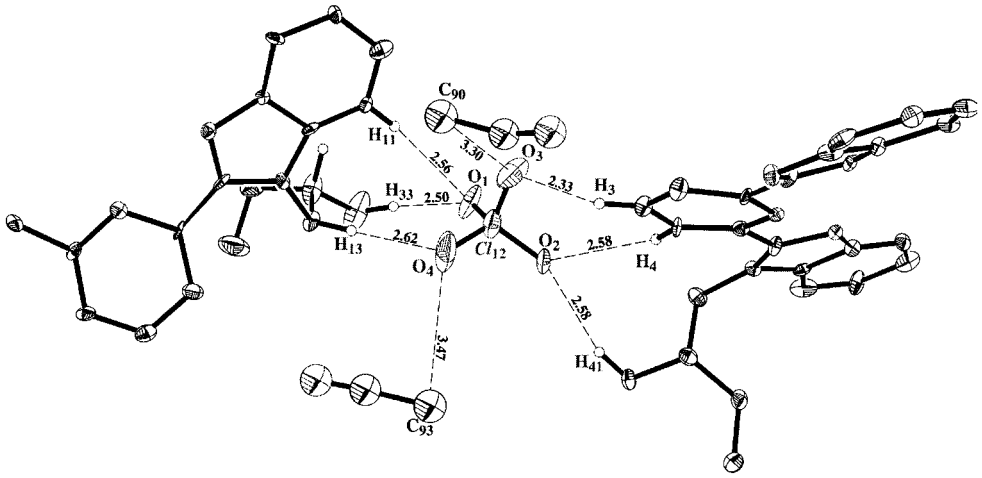

Figure 6. Intermolecular CH···O interactions observed in the crystal structure of $[La(ClO_4)_2(L^{11})_2]_3[La(ClO_4)_2(H_2O)(L^{11})_2](ClO_4)_4 \cdot 15MeCN$ (**1a**). For the sake of clarity, the numbering has been simplified: O_1 = O121, O_2 = O122, O_3 = O123, O_4 = O124, C_{90} = C902, and C_{93} = C935.

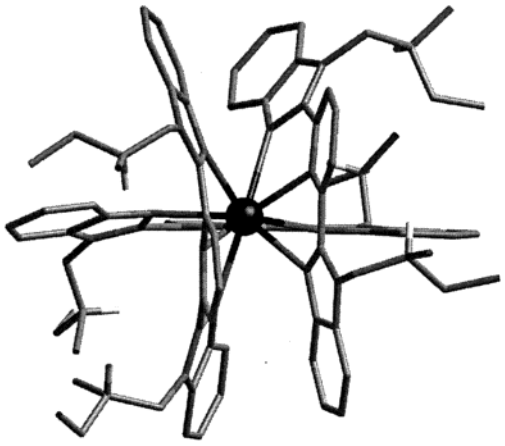

Figure 7. Structure of the $[Eu(L^{11})_3]^{3+}$ cation.

Table 6. Bond Distances (Å) and Angles (deg) in the Coordination Polyhedron of $[Eu(L^{11})_3](ClO_4)_3 \cdot 4.28MeCN$ (**5a**)

Bond Distances					
Eu1−N1A	2.567(6)	Eu1−N2A	2.621(5)	Eu1−N5A	2.591(6)
Eu1−N1B	2.598(5)	Eu1−N2B	2.570(6)	Eu1−N5B	2.609(5)
Eu1−N1C	2.547(6)	Eu1−N2C	2.583(5)	Eu1−N5C	2.573(5)

Bond Angles			
N1A−Eu1−N2A	60.3(2)	N5A−Eu1−N1C	79.4(2)
N1A−Eu1−N5A	65.1(2)	N5A−Eu1−N2C	98.1(2)
N1A−Eu1−N1B	89.8(2)	N5A−Eu1−N5C	73.7(2)
N1A−Eu1−N2B	131.3(2)	N1B−Eu1−N2B	63.9(2)
N1A−Eu1−N5B	69.6(2)	N1B−Eu1−N5B	61.4(2)
N1A−Eu1−N1C	135.1(2)	N1B−Eu1−N1C	135.0(2)
N1A−Eu1−N2C	143.4(2)	N1B−Eu1−N2C	79.0(2)
N1A−Eu1−N5C	79.4(2)	N1B−Eu1−N5C	142.0(2)
N2A−Eu1−N5A	120.2(2)	N2B−Eu1−N5B	120.6(2)
N2A−Eu1−N1B	68.9(2)	N2B−Eu1−N1C	80.6(2)
N2A−Eu1−N2B	71.8(2)	N2B−Eu1−N2C	74.2(2)
N2A−Eu1−N5B	107.0(2)	N2B−Eu1−N5C	96.4(2)
N2A−Eu1−N1C	126.5(2)	N5B−Eu1−N1C	126.5(2)
N2A−Eu1−N2C	140.8(2)	N5B−Eu1−N2C	74.5(2)
N2A−Eu1−N5C	74.2(2)	N5B−Eu1−N5C	141.9(2)
N5A−Eu1−N1B	133.8(2)	N1C−Eu1−N2C	64.8(2)
N5A−Eu1−N2B	160.0(2)	N1C−Eu1−N5C	64.3(2)
N5A−Eu1−N5B	73.3(2)	N2C−Eu1−N5C	129.1(2)

while the third one (molecule C) lies more or less perpendicular to the two others, in contrast with the helical structures we have previously reported for similar complexes.[20] The neopentyl groups lie on the same side of the mean ligand plane in strands A and B, while they are located on both sides of this plane for C. Four of the six neopentyl substituents are disordered, those of ligands A and B occupying two positions with nearly equal populations while those of ligand C have occupancy factors of 0.68 and 0.32. Direct determination of their chirality was therefore not possible; however, an analysis taking into account all the possible combinations of the arm positions showed that all the asymmetric carbon atoms have *S* configuration. Interplanar angles between the pyridine and benzimidazole moieties are dissimilar from one ligand to another: 14.7 and 35° (ligand A), 28 and 29.9° (B), and 0.6 and 20.1° (C), contrary to what is observed for triple helical complexes where the three ligands tend to adopt the same conformation with a mean interplanar angle equal to 25°.[20] As for the 1:2 complex, the crystal packing is governed by CH···O intermolecular interactions (Figure F6 and Table T7 of Supporting Information) involving the noncoordinated perchlorate anions. Each O atom generates two interactions with H atoms located on the benzimidazole groups and the neopentyl arms; two O atoms connect ligands within the same molecule, while the two other ones connect two ligands belonging to two different complex molecules.

Discussion

Solution Behavior. ES-MS, NMR, and spectrophotometric data clearly point to the presence of stable 1:1 and 1:2 complexes with L^{11} in acetonitrile, while the formation of 1:3 complexes appears to be much less favored, consistent with the difficulty of isolating the 1:3 complexes in the solid state. The large discrepancy observed between log K_3 values determined from spectrophotometric and NMR data deserves an explanation. Close examination of spectrophotometric data shows that plots of absorbance vs the ratio $R = [Eu]_t/[L^{11}]_t$ at several wavelengths (Figure F7 of Supporting Information) have essentially one break at $R = 0.5$ (1:2 complex); moreover, the spectra of Figure 3 display an isosbestic point up to the same value of R only. On the other hand, the NMR signals of the 1:2 species (Figure 4) broaden upon addition of more ligand and the signals assigned to the 1:3 species are also quite broad. As has been shown for the triple helical complexes with terpyridine $[Ln(tpy)_3]^{3+}$,[48] this broadening could be due to the partial decomplexation of one ligand molecule in the 1:3 complex, resulting in the formation of conformational isomers in rapid equilibrium; furthermore, the partially decomplexed molecule may also be in rapid exchange with the bulk solvent:

(48) Chapman, R. D.; Loda, R. T.; Riehl, J. P.; Schwartz, R. W. *Inorg. Chem.* **1984**, *23*, 1652−1657.

$$[Ln(L^{11})_3]^{3+} \rightleftharpoons [Ln(L^{11})_2(L^{11})]^{3+}$$

$$[Ln(L^{11})_2(L^{11})]^{3+} + L^{11}* \rightleftharpoons [Ln(L^{11})_2(L^{11*})]^{3+} + L^{11} \quad (4)$$

For terpyridine complexes, however, the dissociation only occurs when water is present in solution.[49] Since we have taken great care to work under anhydrous conditions, we do not favor this explanation but, rather, the following. Complexation usually involves a two-step mechanism with an outer-sphere intermediate:[50]

$$[Ln(L^{11})_2]^{3+} + L^{11} \rightleftharpoons \{[Ln(L^{11})_2](L^{11})]\}^{3+} \rightleftharpoons [Ln(L^{11})_3]^{3+} \quad (5)$$

A close look at the spectrophotometric data reveals that the electronic spectrum of the 1:3 species is very close to the sum of the spectra of the 1:2 species and of the free ligand (Figure 8). Since the outer-sphere interaction does not alter much the electronic properties of the interacting species,[51] we conclude that the data taken into account by the fitting program refer to the outer-sphere species (or to the sum of the outer- and inner-sphere species). On the other hand, in view of the shifts observed, the NMR signals identified for the 1:3 species are those of an inner-sphere complex, which then explains the difference in the calculated stability constants and points to the values determined by NMR corresponding to the true inner-sphere stability constants K_3. Formation of the $[Ln(L^i)_3]^{3+}$ complexes is influenced by the substituents borne by the benzimidazole and central pyridine groups. These substituents can be chosen to tune both the stability of these complexes and the size-discriminating effect along the lanthanide series.[22] With respect to L^1, the introduction of neopentyl groups in L^{11} has a dramatic effect on K_3, reducing its value by about 5 orders of magnitude while K_1 and K_2 are much less affected, being smaller by a little more than 1 order of magnitude. The difficult formation of the tris complexes with L^{11} may be traced back to the steric hindrance generated by the bulky neopentyl substituents, which prevents the intramolecular interstrand π-stacking interactions observed in the closely packed triple-helical structure $[Eu(L^1)_3]^{3+}$. The triple-helical $[Eu(L^1)_3]^{3+}$ structure prevails in the solid state and in solution, but interstrand interactions in solution are maximum for Gd(III) ($\log K_3 = 6.6$) while the stability of the Lu(III) triple helical compound is much weaker ($\log K_3 = 2.7$), as similarly found with ligands L^4 and L^8.[22] In our case, the Lu(III) 1:3 complex could not be evidenced at all.

Structural Aspects. In **1a**, The La−N(py) distances span the range 2.71−2.79 Å in the two complex cations with an average of 2.75(3) Å, substantially longer than the La−N(bz) mean bond length (2.66(3) Å), reflecting a compromise between the constrained bite angle of the ligand and the size of the entering metal ion.[16] As far as the perchlorate anions are concerned, the Ln−O(b) distance in $[La(ClO_4)_2(H_2O)(L^{11})_2]^+$ is slightly longer than in $[La(ClO_4)_2(L^{11})_2]^+$, but the La−O(m) contact is much shorter, by 0.1 Å. This short distance is compensated by a relatively long La−O(w) bond length, 2.65 Å, compared to 2.29 Å in $[Lu(L^1)_2(MeOH)(H_2O)]^{3+}$ [20] (the ionic radius of Lu(III) is 0.19 Å smaller than that of La(III)[13]), which is probably due to the H-bond interaction with the bound O atom from the monodentate perchlorate ion. The bidentate perchlorates bound to the metal ion have approximate C_{2v} symmetry, and the Cl−O(b) distances are slightly longer (1.45(2) Å) than the Cl−O bond lengths involving noncoordinating O atoms (1.42(2) Å); both distances are longer than those found in ionic perchlorates (1.39(5) Å), which have approximate tetrahedral symmetry. The monodentate perchlorate has rough C_{3v} symmetry, and the bound O atom is further implied in an intramolecular H bond with the coordinated water molecule, resulting in a Cl−O(m) distance of 1.40(1) Å, a value between the average Cl−O bond lengths of bidentate anions and the bond lengths of noncoordinated anions. In **5a**, the Eu−N distances are in the range 2.55−2.62 Å (mean 2.58(1) Å) with no clear-cut difference between Eu−N(py) and Eu−N(bz) on one hand and between the ligand molecules on the other hand.

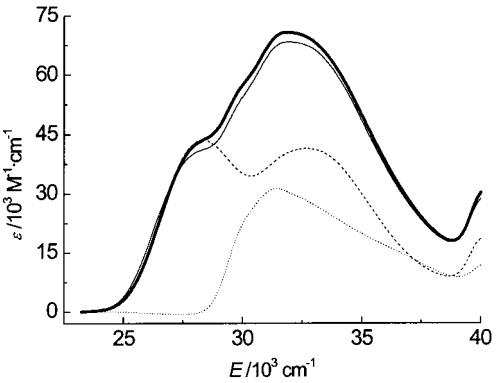

Figure 8. Electronic spectra extracted from the titration of L^{11} by Eu(Otf)$_3$: ligand L^{11} (dotted line); 1:2 complex (dashed line); 1:3 complex (solid line); sum of L^{11} and 1:2 (bold line).

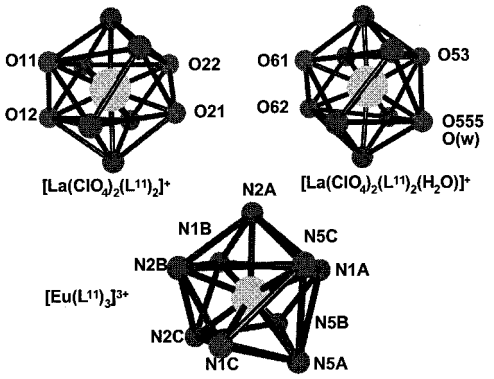

Figure 9. Coordination polyhedra around Ln(III) ions.

While the coordination polyhedra of the bis complexes of L^1 with octadentate Yb(III)[22] and Lu(III)[20] are derived from cubic arrangements, those of the two 10-coordinate La(III) ions in $[La(ClO_4)_2(L^{11})_2]^+$ and $[La(ClO_4)_2(H_2O)(L^{11})_2]^+$ can be described as distorted capped square antiprisms (1:4:4:1 polyhedra, Figure 9).[52] The capping atoms are the N atoms from the pyridines, and the two planes are defined by two O atoms from the perchlorate anions and two N atoms from the benzimidazole groups. In $[La(ClO_4)_2(H_2O)(L^{11})_2]^+$, one O atom of one plane comes from the water molecule. In fact the partial decomplexation of one bidentate perchlorate anion allowing water to enter the inner coordination sphere does not induce large changes in the surroundings of the metal ion, but for a slight expansion of the coordination sphere (Table 7). Contrary to the coordination polyhedra in $[Ln(L^i)_3]^{3+}$ for $i = 1$[20] and 5,[21] the inner

(49) Mallet, C.; Thummel, R. P.; Hery, C. *Inorg. Chim. Acta* **1993**, *210*, 223−231.
(50) Wilkins, R. G. *Kinetics and Mechanisms of Reaction of Transition Metal Complexes*; VCH: Weinheim, 1991.
(51) Choppin, G. R.; Henrie, D. E.; Buijs, K. *Inorg. Chem.* **1966**, *5*, 1743−1748.
(52) Xu, J. D.; Radkov, E.; Ziegler, M.; Raymond, K. N. *Inorg. Chem.* **2000**, *39*, 4156−4164.

Table 7. Ln−X Mean Distances (Å) and Effective Ionic Radii r_i (Å) in 1:2 and 1:3 Complexes

complex	NC	Ln−N pyridine	Ln−N benzimidazole	Ln−O	r_i[a]
$[La(L^{11})_2(ClO_4)_2]^+$	10	2.75(3)	2.64(2), 2.64(2)	2.66(2)	1.28
$[La(L^{11})_2(ClO_4)_2(H_2O)]^+$	10	2.76(1)	2.69(1), 2.69(1)	2.68(1), 2.584(1), 2.654(1)	1.29
$[Yb(L^1)_2(OH)]_2^{4+}$ [22]	8	2.46(3)	2.44(2), 2.55(1)	2.23(1)	1.005
$[Lu(L^1)_2(MeOH)(H_2O)]^{3+}$ [20]	8	2.44(1)	2.37(0), 2.45(1)	2.35(1), 2.29(1)	0.985
$[Eu(L^{11})_3]^{3+}$	9	2.57(2)	2.59(2)		1.12
$[Eu(L^1)_3]^{3+}$ [20]	9	2.58(1)	2.60(1)		1.13
$[Eu(L^5)_3]^{3+}$ [21]	9	2.56(3)	2.60(3)		1.13
$[Eu(terpy)_3]^{3+}$ [56]	9	2.55(1)[b]	2.59(2)[c]		1.12

[a] According to Shannon[57] with $r(O) = 1.31$ Å and $r(N) = 1.46$ Å. Mean values reported in the literature amount to 1.12, 1.18, and 1.27 Å for nonacoordinate Eu(III), decacoordinate Eu(III), and decacoordinate La(III), respectively.[57] [b] Eu−N(central pyridine) distances. [c] Eu−N(distal pyridine) distances.

coordination sphere in $[Ln(L^{11})_3]^{3+}$ (Figure 9) is very distorted with respect to the idealized tricapped trigonal prismatic geometry (ttp). This distortion has been investigated using the geometrical analysis proposed earlier[21] where the pseudo-tricapped-trigonal prism around the Eu(III) ion is considered as the superposition of three tripods defined by the following N atoms of the coordinated ligands (Figure F8 and Table T8 of Supporting Information): N2A, N2B, N2C (superior tripod, s), N5A, N5B, N5C (inferior tripod, i), and N1A, N1B, N1C (central tripod, c). The two distal tripods are relatively well aligned along the pseudo-C_3 axis, but the angles θ_i between individual vectors Eu−N2A, Eu−N2B, and Eu−N2C and their sum R^1 = Eu−N2A + Eu−N2B + Eu−N2C on one hand and the vectors Eu−N5A, Eu−N5B, and Eu−N5C and their sum R^2 = Eu−N5A + Eu−N5B + Eu−N5C on the other hand differ widely. These angles define the flattening of the trigonal prism along the C_3 axis and vary between 11.7° and 72.5° in the investigated complex, while they are in the range 46−49° for $[Eu(L^5)_3]^{3+}$ and are all equal to 55° in $[Eu(L^1)_3]^{3+}$. Interestingly, ligands A and B display two very different angles, $\theta_1 = 70.2°$, $\theta_2 = 11.7°$ for A and $\theta_1 = 11.9°$, $\theta_2 = 71.3°$ for B, while ligand C has two similar angles, 71.3° and 72.5°. This means that ligands A and B are mirror images of each other, with opposite rotation of the two ligand strands with respect to the pseudo-C_3 axis. The other geometric parameters of this analysis confirm the large deviation of the coordination polyhedron of $[Eu(L^{11})_3]^{3+}$ with respect to the ttp geometry, which is not suitable for describing the metal ion environment (no other idealized geometry could be found that fits the coordination polyhedron).

Conclusion

The introduction of neopentyl groups onto the benzimidazole sidearms of ligand L^{11} has a profound effect on the formation and structure of the triple helical complexes $[Ln(L^{11})_3]^{3+}$. In solution, the third ligand penetrates with difficulty into the inner coordination sphere and the corresponding third successive stability constants are small ($\log K_3 \approx 1$) for La(III) and Eu(III), while no tris complex is seen for Lu(III), even in the presence of a large excess of ligand. In contrast, large but flatter substituents such as dimethoxybenzyl groups in L^4 have a less drastic effect, $\log K_3$ being around 3 for Ce(III)−Lu(III). A clue for understanding these effects comes from the crystal structure determinations of the triple helical complexes with L^1, L^5, L^8, and L^{11}. Alkyl N-substituents have a large influence on the site symmetry of the metal ion, which decreases from pseudo-D_3 in the triple helical complex with L^1 to pseudo-C_3 in $[Eu(L^5)_3]^{3+}$ and to C_1 in $[Eu(L^{11})_3]^{3+}$, a fact confirmed by high-resolution luminescence measurements.[53] The steric hindrance of the neopentyl groups generates a positioning of ligands L^{11} around the metal ion such that the stabilizing interstrand π-stacking interactions evidenced in $[Eu(L^1)_3]^{3+}$ [20] are lost. This is not the case in $[Eu(L^8)_3]^{3+}$ where the dimethoxybenzyl groups do not exclude such interactions from occurring in the solid state.[45] Therefore, this study demonstrates that in addition to the electronic effects that can be modulated by specific substituents bound to the central pyridine ring in triple-helical $[Ln(L^i)_3]^{3+}$ entities,[45,54] steric effects induced by substituted benzimidazole sidearms can be used for improving the design of such complexes. Substitution at the 4-position of the benzimidazole rings prevents complexation, while substitution at the 5-position in L^5 has only minor thermodynamic and structural consequences.[45] The connection of alkyl groups of increasing size at the 1-position on going from L^1 (R^2 = Me)[45] to L^2 (R^2 = Et),[45] L^4 (R^2 = $((CH_3O)_2C_6H_4CH_2)$,[45] and eventually L^{11} (R^2 = neopentyl) gradually limits intramolecular interstrand π-stacking in triple-helical complexes $[Ln(L^i)_3]^{3+}$, thus affecting thermodynamic stability, selectivity, and structural features. This complete investigation of a series of lanthanide-containing triple-helical complexes illustrates one of the rare cases for which the relative importance of electronic and steric effects is unambiguously established, a crucial point for "programming" functional lanthanide complexes.[55]

Acknowledgment. We gratefully acknowledge D. Baumann and V. Foiret for their technical assistance. We thank Prof. Pierre Vogel for the use of his polarimeter. This work is supported through grants from the Swiss National Science Foundation.

Supporting Information Available: Table T1 with elemental analysis of L^{11} and its 1:2 and 1:3 complexes, Tables T2 and T3 with selected bond lengths, angles, and least-squares plane data for L^{11}, Tables T4−T7 with interplanar angles and intermolecular interactions in **1a** and **5a**, Table T8 with the geometrical analysis of the inner coordination sphere in $[Eu(L^i)_3]^{3+}$, Figure F1 with the ^{1}H NMR spectrum of L^{11}, Figure F2 with intermolecular interactions in **5a**, Figure F3 with ES-MS spectra of the system Eu^{3+}/L^{11}, Figures F4 and F5 showing the structure and atom-numbering scheme for **1a** and **5a**, Figure F6 with CH···O intermolecular interactions in **5a**, Figure F7 with absorption plots, Figure F8 defining vectors and angles for the geometrical analysis of **5a**. This material is available free of charge via the Internet at http://pubs.acs.org.

IC001289O

(53) Muller, G. Ph.D. Dissertation, University of Lausanne, Lausanne, Switzerland, 2000.
(54) Bochet, C. G.; Piguet, C.; Williams, A. F. *Helv. Chim. Acta* **1993**, *76*, 372−384.
(55) Piguet, C.; Bünzli, J.-C. G. *Chimia* **1998**, *52*, 579−584.
(56) Semenova, L. I.; Sobolev, A. N.; Skelton, B. W.; White, A. H. *Aust. J. Chem.* **1999**, *52*, 519−529.
(57) Shannon, R. D. *Acta Crystallogr.* **1976**, *A32*, 751−767.